LULEÅ UNIVERSITY OF TECHNOLOGY

Research Report

Derivation of MNA Circuit Equations for the PEEC Method

September, 2003
Jonas.Ekman@sm.luth.se

LULEÅ UNIVERSITY OF TECHNOLOGY

Research Report

Introduction

This report details the derivation of the MNA equations used for Partial Element Equivalent Circuit analysis. When using the MNA method for circuit analysis, voltages and currents are calculated at the same time from a sparse system matrix, $\mathbf{A}$, by solving the linear system

$$\mathbf{A}\,\mathbf{x} = \mathbf{b} \tag{1}$$

where $\mathbf{x}$ include the current (in time) node voltages and branch currents and $\mathbf{b}$ include the source terms.

Derivation of MNA PEEC Circuit Equations

The derivation of the circuit equations start by considering the three bodies, i, j, and k, in Fig. 1 and the relationship

$$\mathbf{V} = \mathbf{P}\,\mathbf{Q} \tag{2}$$

where $\mathbf{V}$ is the potential vector (to infinity), $\mathbf{P}$, the coefficient of potential matrix, $\mathbf{Q}$ is the charge vector for the patches.

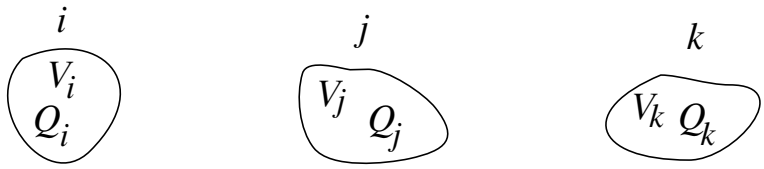

Figure 1: Three bodies with individual potential and charge.

Considering only the first patch, i, gives the following equation

$$V_i = P_{ii}Q_i + P_{ij}Q_j + P_{ik}Q_k \tag{3}$$

which can be rewritten as

$$\frac{V_i}{P_{ii}} = Q_i + \frac{P_{ij}}{P_{ii}}Q_j + \frac{P_{ik}}{P_{ii}}Q_k \tag{4}$$

where $P_{\alpha\beta}$ is the mutual coefficient of potential (describing the electric field coupling between electrically charged bodies), $P_{\alpha\alpha}$ is the self coefficient of potential (relating the potential to the charge of a body), and $\alpha, \beta = i, j, k$.

Assuming a sinusoidal steady-state condition at the frequency $f = 2\pi\omega$, Eq. (4) can be written as

$$j\omega\frac{1}{P_{ii}}V_i = j\omega Q_i + j\omega\frac{P_{ij}}{P_{ii}}e^{-j\omega\tau_{ij}}Q_j + j\omega\frac{P_{ik}}{P_{ii}}e^{-j\omega\tau_{ik}}Q_k \tag{5}$$

Where the exponential term $e^{-j\omega\tau}$ describes time retardation, equal to a phase shift in the frequency domain, between two patches. By introducing the notation

$$I_{C_\alpha} = j\omega Q_\alpha \tag{6}$$

for the current leaving the corresponding body where $\alpha = i, j, k$, Eq. (5) ca be written as

$$j\omega \frac{1}{P_{ii}} V_i = I_{C_i} + \frac{P_{ij}}{P_{ii}} e^{-j\omega\tau_{ij}} I_{C_j} + \frac{P_{ik}}{P_{ii}} e^{-j\omega\tau_{ik}} I_{C_k} \tag{7}$$

and Fig. 1 is updated to Fig. 2.

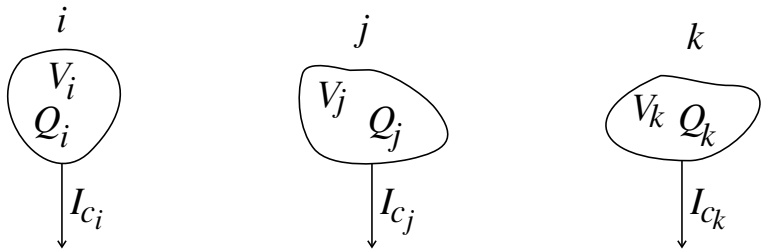

Figure 2: Three bodies with indicated current components.

By rearranging Eq. (7) into

$$I_{C_i} = j\omega \frac{1}{P_{ii}} V_i + \frac{P_{ij}}{P_{ii}} e^{-j\omega\tau_{ij}} I_{C_j} + \frac{P_{ik}}{P_{ii}} e^{-j\omega\tau_{ik}} I_{C_k} \tag{8}$$

enables the construction of an equivalent circuit according to with the retarded current controlled

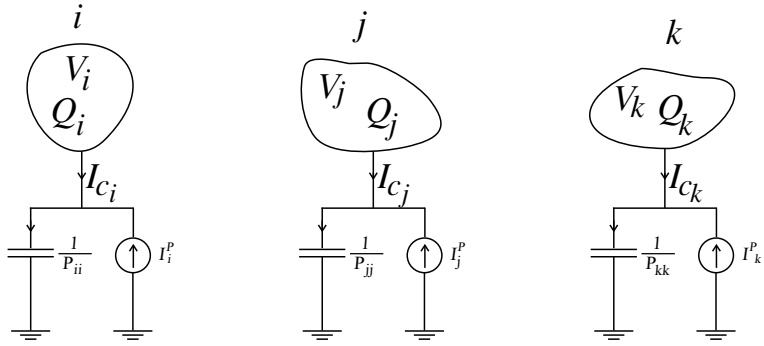

Figure 3: Three bodies with indicated current components.

current sources described as

$$I_{C_\alpha} = \frac{P_{\alpha\beta}}{P_{\alpha\alpha}} e^{-j\omega\tau_{\alpha\beta}} I_{C_\beta} + \frac{P_{\alpha\gamma}}{P_{\alpha\alpha}} e^{-j\omega\tau_{\alpha\gamma}} I_{C_\gamma} \tag{9}$$

and the notation *pseudo-capacitance* for the term $j\omega\frac{1}{P_{ii}}V_i$ as introduced in [1].

Applying the derived equations for the PEEC method allows the writing of the systems of equation of the type in Eq. (8) in matrix form since the PEEC model cell has a well known structure. The matrix notation is then

$$\mathbf{I}_C \;=\; j\omega\mathbf{F}\mathbf{V} \;-\; \mathbf{S}'\mathbf{I}_C \tag{10}$$

where $\mathbf{I}_C$ is the patch current vector, $\mathbf{F}$ is a $n_c \times n_c$ matrix with elements of the type $F_{ii} = \frac{1}{P_{ii}}$, $\mathbf{V}$ is the patch potential vector, $\mathbf{S}'$ is a $n_c \times n_c$ matrix with elements of the type $S'_{\alpha\beta} = \frac{P_{\alpha\beta}}{P_{\alpha\alpha}}$ and $\alpha \neq \beta$, and n_c is the total number of charged bodies.

The three bodies, i, j, k, in the previous figures can in the PEEC method describe the charge distribution on different discretized parts of the same conductor between which we have conduction and polarization currents flowing. This assumption requires the previous figures to be updated according to.

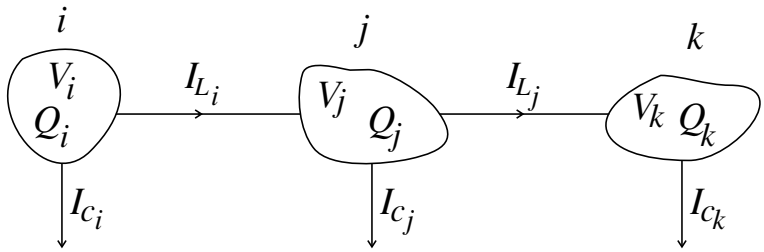

Figure 4: Three bodies with indicated current components.

The structure of the basic PEEC cell enables a matrix formulation of the relationship between $\mathbf{I}_C$ and $\mathbf{I}_L$ for a complete structure since

$$\left\{ \begin{array}{rcrr} I_{C_i} & = & -I_{L_i} & \\ I_{C_j} & = & I_{L_i} & -I_{L_j} \\ I_{C_k} & = & & I_{L_j} \end{array} \right. \tag{11}$$

Then the relationship $\mathbf{I}_C = \mathbf{A}^T\mathbf{I}_L$ is obtained by defining a $n_C \times n_L$ connectivity matrix $\mathbf{A}$ describing the currents leaving and entering each node and n_L is the number of cells between

the charged bodies. In this case $n_C = 3$, $n_L = 2$, and

$$\mathbf{A} = \begin{bmatrix} -1 & 1 & 0 \\ 0 & -1 & 1 \end{bmatrix} \tag{12}$$

The usage of inter-cell currents $\mathbf{I}_L$ enables the modeling of the magnetic coupling effects as will be shown later and transforms Eq. (10) into

$$\mathbf{A}^T\mathbf{I}_L = j\omega\mathbf{FV} - \mathbf{S}'\mathbf{A}^T\mathbf{I}_L \tag{13}$$

Which enables the construction of a matrix taking to account all electric effects as

$$\mathbf{S} = \mathbf{S}' + \mathbf{1} \tag{14}$$

where $\mathbf{1}$ is the identity matrix. This results in the $\mathbf{S}$ matrix which is of dimension $n_c \times n_c$ with elements of the type $S_{\alpha\beta} = \frac{P_{\alpha\beta}}{P_{\alpha\alpha}}$, $\forall\alpha, \beta$. And Eq. (13) can be written as

$$j\omega\mathbf{FV} - \mathbf{SA}^T\mathbf{I}_L = \mathbf{0} \tag{15}$$

The inclusion of an external current source(s) exciting one (or more) charged bodies requires the updating of Fig. 4 into The addition of an external current source under the previous assump-

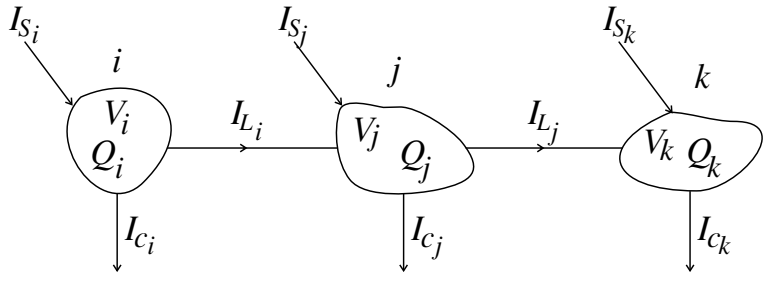

Figure 5: Three bodies with external source terms.

tions effects the charge of the directly excited patch, but also the charges of the surrounding patched (through the mutual electric field coupling effects described by the coefficients of potentials). This results in the relationship between the equivalent circuit source vector $\mathbf{I}_{S_{Eq}}$ and the source vector $\mathbf{I}_S$ according to

$$\mathbf{I}_{S_{Eq}} = \mathbf{SI}_S \tag{16}$$

where the vector $\mathbf{I}_S$ is of size n_c and a nonzero entry at position n indicates a current injected into node n. For a PEEC model without electric field coupling $\mathbf{I}_{S_{Eq}} = \mathbf{I}_S$. The source term is included in Eq. (15) at the RHS resulting in

$$j\omega\mathbf{F}\mathbf{V} - \mathbf{S}\mathbf{A}^T\mathbf{I}_L = \mathbf{S}\mathbf{I}_S \tag{17}$$

The Kirchoffs voltage law (KVL) applied to the basic structure of the PEEC cell produces an equation system according to

$$-\mathbf{A}\mathbf{V} - (\mathbf{R} + j\omega\mathbf{L})\mathbf{I}_L = \mathbf{V}_S \tag{18}$$

where $\mathbf{R}$ is a diagonal matrix containing the d.c. resistance between the nodes, $\mathbf{L}$ contains the partial inductances [2, 3], and $\mathbf{V}_S$ is a voltage source excitation vector. The combination of Eq. (17) and (18) in one equation system results in

$$\begin{bmatrix} -\mathbf{A} & -(\mathbf{R} + j\omega\mathbf{L}) \\ j\omega\mathbf{F} + \mathbf{S}\mathbf{Y}_L & -\mathbf{S}\mathbf{A}^T \end{bmatrix} \begin{bmatrix} \mathbf{V} \\ \mathbf{I}_L \end{bmatrix} = \begin{bmatrix} \mathbf{V}_S \\ \mathbf{S}\mathbf{I}_S \end{bmatrix} \tag{19}$$

where a admittance matrix $\mathbf{Y}_L$ describing the lumped elements have been included. The equations in (19) is refereed to as the modified nodal analysis (MNA) equation system as presented in [4, 5, 6, 7].

Time Domain MNA Equation System

The time domain equations for the solution of PEEC model problems can be derived in the same way as for the frequency domain. The difference is the inclusion of the time retardation that is expressed as a complex part in the partial mutual couplings for frequency domain models, Eq. (20), while for time domain PEEC models the retardation is written as a finite time delay, Eq. (21). The two equations below Eq. (20) and (21), displays the induced voltage in cell α due to the magnetic field coupling with cell β.

$$V_{\alpha\beta} = j\omega Lp_{\alpha\beta}\, I_\beta\, e^{-j\omega\tau_{\alpha\beta}} \tag{20}$$

$$v_{\alpha\beta} = Lp_{\alpha\beta}\, \frac{di_\beta(t - \tau_{\alpha\beta})}{dt} \tag{21}$$

Static MNA Equations

For static time domain PEEC models, the MNA system can be written as

$$\begin{bmatrix} -\mathbf{A} & -(\mathbf{R}+\mathbf{L}\frac{d}{dt}) \\ \mathbf{F}\frac{d}{dt}+\mathbf{S}\mathbf{Y}_L & -\mathbf{S}\mathbf{A}^T \end{bmatrix} \begin{bmatrix} \mathbf{V} \\ \mathbf{I}_L \end{bmatrix} = \begin{bmatrix} \mathbf{V}_S \\ \mathbf{S}\mathbf{I}_S \end{bmatrix} \tag{22}$$

Discretizing matrix Eq. (22) in time by using the Backward Euler (BE) scheme yields

$$\begin{bmatrix} -\mathbf{A} & -(\mathbf{R}+\mathbf{L}\frac{1}{dt}) \\ \mathbf{F}\frac{1}{dt}+\mathbf{S}\mathbf{Y}_L & -\mathbf{S}\mathbf{A}^T \end{bmatrix} \begin{bmatrix} \mathbf{V}_n \\ \mathbf{I}_{nL} \end{bmatrix} = \begin{bmatrix} \mathbf{V}_S - \mathbf{L}\frac{1}{dt}\mathbf{I}_{n-1_L} \\ \mathbf{S}\mathbf{I}_S + \mathbf{F}\frac{1}{dt}\mathbf{V}_{n-1} \end{bmatrix} \tag{23}$$

where for a fixed time step, dt, the leftmost block only has to be calculated once.

Full-wave MNA Equations

The full-wave solution of PEEC models must include the time retarded electric- and magnetic-field couplings. The frequency domain representation through complex mutual partial elements must be converted to individual time delays in the time domain. This results in real valued matrix entries in the **L** and **S**-matrices and the delayed coupling of the corresponding currents and/or potentials. Comparing the electric field coupling for the time- and frequency-domain for a PEEC one-cell shows the difference.

$$\begin{array}{lcccc} \textit{Frequendy domain} \rightarrow & Lp_{\alpha\beta} & e^{-j\omega\tau_{\alpha\beta}} & j\omega & I_\beta(\omega) \\ \textit{Time domain} \rightarrow & Lp_{\alpha\beta} & & \frac{d}{dt} & i_\beta(t-\tau_{\alpha\beta}) \end{array}$$

As can be seen, the time retardation expressed as a phase shift incorporated in the (complex) mutual partial elements in the FD is expressed as a real time retardation in the coupled current in the TD. This implies that each mutual partial element has its own coupled current(s) due to the different delay times, and the matrix-vector-products, involving the **L**- and **S**-matrices, in the previous equations are converted to matrix(row)-matrix(column)-products in the full-wave time domain formulation.

Since the self terms in the **L**- and **S**-matrices are not retarded the derivation of the full-wave equations is simplified if the self terms are separated from the mutual terms in the **L**- and **S**-matrices according to

$$\mathbf{L} = \mathbf{L}_S + \mathbf{L}_M \tag{24}$$

$$\mathbf{S} = \mathbf{S}_S + \mathbf{S}_M \tag{25}$$

Theoretically since all electric field couplings are delayed the $\mathbf{S}_S$ matrix would reduce to the identity matrix **1**. However, the finite time step used in the integration routine force some

electric field couplings to be considered to be instantaneous, ie $\tau_{\alpha\beta} < T_{step}$. This result in the moving of the instantaneous couplings in the $\mathbf{S}_M$ matrix to the corresponding location in the $\mathbf{S}_S$ matrix. Substituting Eq. (24) and (25) into (22) yields

$$\begin{bmatrix} -\mathbf{A} & -(\mathbf{R} + (\mathbf{L}_S + \mathbf{L}_M)\frac{d}{dt}) \\ \mathbf{F}\frac{d}{dt} + (\mathbf{S}_S + \mathbf{S}_M)\mathbf{Y}_L & -(\mathbf{S}_S + \mathbf{S}_M)\mathbf{A}^T \end{bmatrix} \begin{bmatrix} \mathbf{V} \\ \mathbf{I}_L \end{bmatrix} = \begin{bmatrix} \mathbf{V}_S \\ (\mathbf{S}_S + \mathbf{S}_M)\mathbf{I}_S \end{bmatrix} \tag{26}$$

Since the mutual coupled terms depend on previous node voltages and branch currents they are considered to be known and therefore moved to the RHS resulting in

$$\begin{bmatrix} -\mathbf{A} & -(\mathbf{R} + \mathbf{L}_S\frac{d}{dt}) \\ \mathbf{F}\frac{d}{dt} + \mathbf{S}_S\mathbf{Y}_L & -\mathbf{S}_S\mathbf{A}^T \end{bmatrix} \begin{bmatrix} \mathbf{V}(t) \\ \mathbf{I}_L(t) \end{bmatrix} = \tag{27}$$

$$\begin{bmatrix} \mathbf{V}_S + \mathbf{L}_M\frac{d}{dt}\mathbf{I}_L(t-\tau) \\ \mathbf{S}_S\mathbf{I}_S(t) + \mathbf{S}_M\mathbf{I}_S(t-\tau) - \mathbf{S}_M\mathbf{Y}_L\mathbf{V}(t-\tau) + \mathbf{S}_M\mathbf{A}^T\mathbf{I}_L(t-\tau) \end{bmatrix}$$

Discretizing Eq. (27) using the Backward Euler, as in Eq. (23), results in

$$\begin{bmatrix} -\mathbf{A} & -(\mathbf{R} + \mathbf{L}_S\frac{1}{dt}) \\ \mathbf{F}\frac{1}{dt} + \mathbf{S}_S\mathbf{Y}_L & -\mathbf{S}_S\mathbf{A}^T \end{bmatrix} \begin{bmatrix} \mathbf{V}_n(t) \\ \mathbf{I}_{n_L}(t) \end{bmatrix} = \tag{28}$$

$$\begin{bmatrix} \mathbf{V}_S - \mathbf{L}_S\frac{1}{dt}\mathbf{I}_{n-1_L}(t) + \mathbf{L}_M\frac{1}{dt}\left[\mathbf{I}_{n_L}(t-\tau) - \mathbf{I}_{n-1_L}(t-\tau)\right] \\ \mathbf{S}_S\mathbf{I}_S(t) + \mathbf{F}\frac{1}{dt}\mathbf{V}_{n-1}(t) + \mathbf{S}_M\mathbf{I}_S(t-\tau) - \mathbf{S}_M\mathbf{Y}_L\mathbf{V}(t-\tau) + \mathbf{S}_M\mathbf{A}^T\mathbf{I}_{n_L}(t-\tau) \end{bmatrix}$$

where $\mathbf{V}_n(t)$, $\mathbf{V}_{n-1}(t)$, $\mathbf{I}_{n_L}(t)$, and $\mathbf{I}_{n-1_L}(t)$ is the same as in Eq. (23) detailing the electromagnetic quasi-static solution. The full-wave solution in Eq. (28) requires the storage of previous nodal voltages $\mathbf{V}(t)$, branch currents $\mathbf{I}_L(t)$, and current source excitation $\mathbf{I}_S(t)$ to enable the evaluation of the individually retarded electric and magnetic coupling terms. More specifically the retarded nodal voltages-, branch currents-, and source current vectors transforms to matrices for the full-wave case, resulting in the following matrices ***for each instant in time***

$$\mathbf{I}_{n_L}(t-\tau) = \begin{bmatrix} 0 & I_{n_1}(t-\tau_{21}) & . & . & I_{n_1}(t-\tau_{nc1}) \\ I_{n_2}(t-\tau_{12}) & 0 & . & . & I_{n_2}(t-\tau_{nc2}) \\ . & . & . & . & . \\ . & . & . & . & . \\ I_{n_{n_c}}(t-\tau_{1nc}) & I_{n_{nc}}(t-\tau_{2nc}) & . & . & 0 \end{bmatrix} \tag{29}$$

$$\mathbf{I}_{n-1_L}(t-\tau) = \begin{bmatrix} 0 & I_{n-1_1}(t-\tau_{21}) & . & . & I_{n-1_1}(t-\tau_{nc1}) \\ I_{n-1_2}(t-\tau_{12}) & 0 & . & . & I_{n-1_2}(t-\tau_{nc2}) \\ . & . & . & . & . \\ . & . & . & . & . \\ I_{n-1_{nc}}(t-\tau_{1nc}) & I_{n-1_{nc}}(t-\tau_{2nc}) & . & . & 0 \end{bmatrix} \tag{30}$$

that is used with the mutual partial inductance matrix, $\mathbf{L}_M$ in a column- (for the $\mathbf{I}_{n_L}(t-\tau)$, $\mathbf{I}_{n-1_L}(t-\tau)$ matrices) row- (for the $\mathbf{L}_M$ matrix) wise multiplication to obtain the correct retarded magnetic field couplings of the form

$$Lp_{12}\,\frac{1}{dt}\,\left[I_{n_2}(t-\tau_{12}) - I_{n-1_2}(t-\tau_{12})\right] \tag{31}$$

Further, the $\mathbf{I}_S(t-\tau)$ matrix is constructed in the same way resulting in

$$\mathbf{I}_S(t-\tau) = \begin{bmatrix} 0 & I_S(t-\tau_{21}) & . & . & I_S(t-\tau_{nc1}) \\ I_S(t-\tau_{12}) & 0 & . & . & I_S(t-\tau_{nc2}) \\ . & . & . & . & . \\ . & . & . & . & . \\ I_S(t-\tau_{1nc}) & I_S(t-\tau_{2nc}) & . & . & 0 \end{bmatrix} \tag{32}$$

that is used with the mutual partial normalized coefficient of potential matrix, $\mathbf{S}_M$ in a column- (for the $\mathbf{I}_S(t-\tau)$ matrix) row- (for the $\mathbf{M}_M$ matrix) wise multiplication to obtain the correct retarded source couplings of the form

$$\frac{P_{12}}{P_{11}}\,I_S(t-\tau_{12}) + \frac{P_{13}}{P_{11}}\,I_S(t-\tau_{13}) + \ ... \tag{33}$$

The inclusion of lumped resistances eliminates the term $\mathbf{S}_M\mathbf{Y}_L\mathbf{V}(t-\tau)$ from the RHS since the resistive effects are instantaneous. But, for charge- and current- storing lumped components the retarded effects has to be taken into account.

Numerical Experiments

The derived MNA equations has been implemented in a C++ based 3D PEEC solver and tested using the transmission line geometry depicted in Fig. 6. The results in Fig. 7 and 8 has been

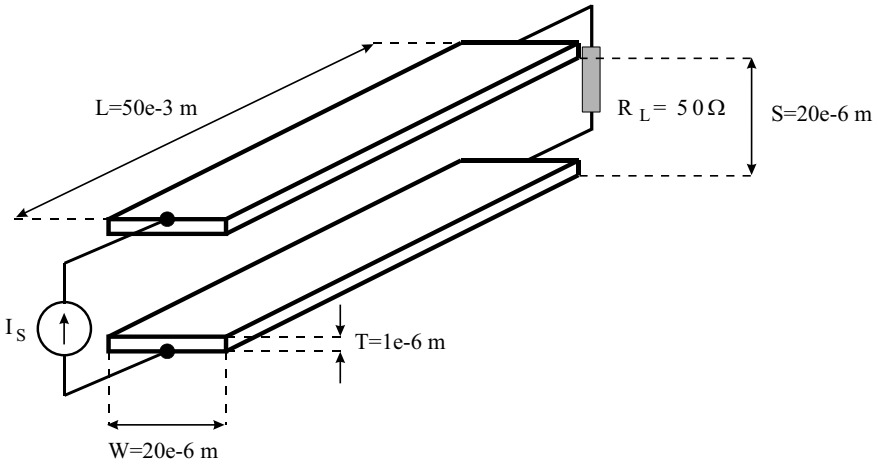

Figure 6: Transmission line geometry used for numerical experiments.

verified using a combined PSpice lossy transmission line simulation for which the transmission line parameters has been extracted using a 2D program, LinPar for Windows ver. 1.0 [8]. The results are for a single pulse with rise time = fall time = 100ps, pulse width = 1.9ns, current amplitude = 2mA, and the time step used in the simulations = 2ps.

(L, P, R, τ)PEEC Simulation

Fig. 7 results are for 40 inductive cells in the length direction and 0 (zero) inductive cells for the width and thickness directions.

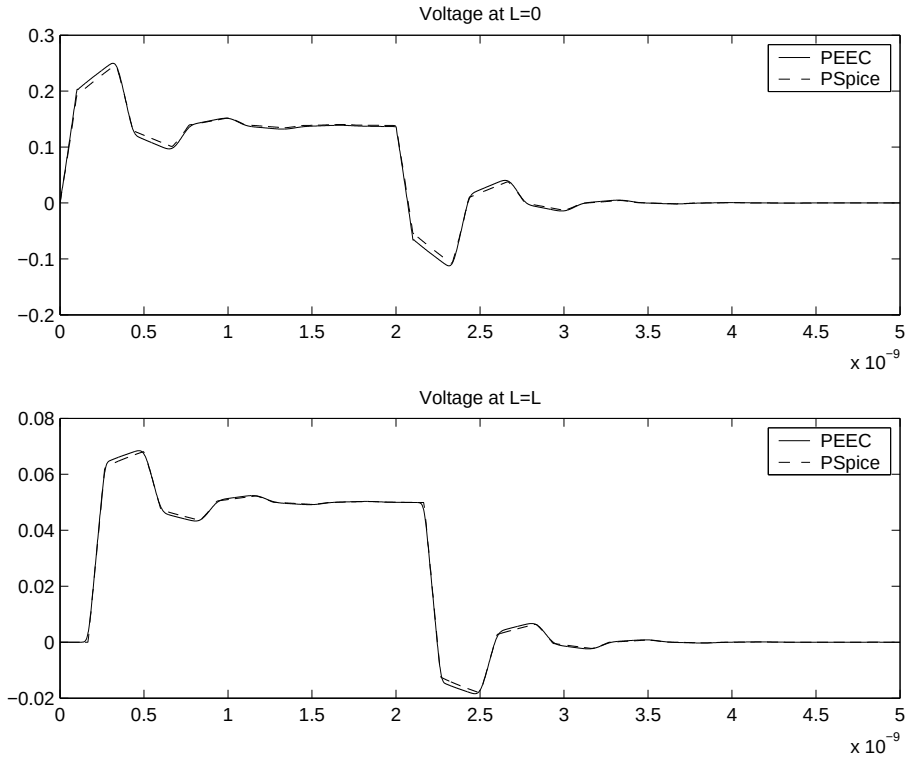

Figure 7: Near- and far-end response for TL. (L, P, R, τ)PEEC simulation.

The results are very good for this simple PEEC model, requiring no more than 3 seconds per time step.

(L, P, R, τ, VFI)PEEC Simulation

To account for the Skin effect and thereby improve the accuracy compared to PSpice results, a simulation using 20 inductive cells in the length, 10 inductive cells in the width, and 0 (zero) inductive cells in the thickness direction was used. The results are shown in Fig. 8

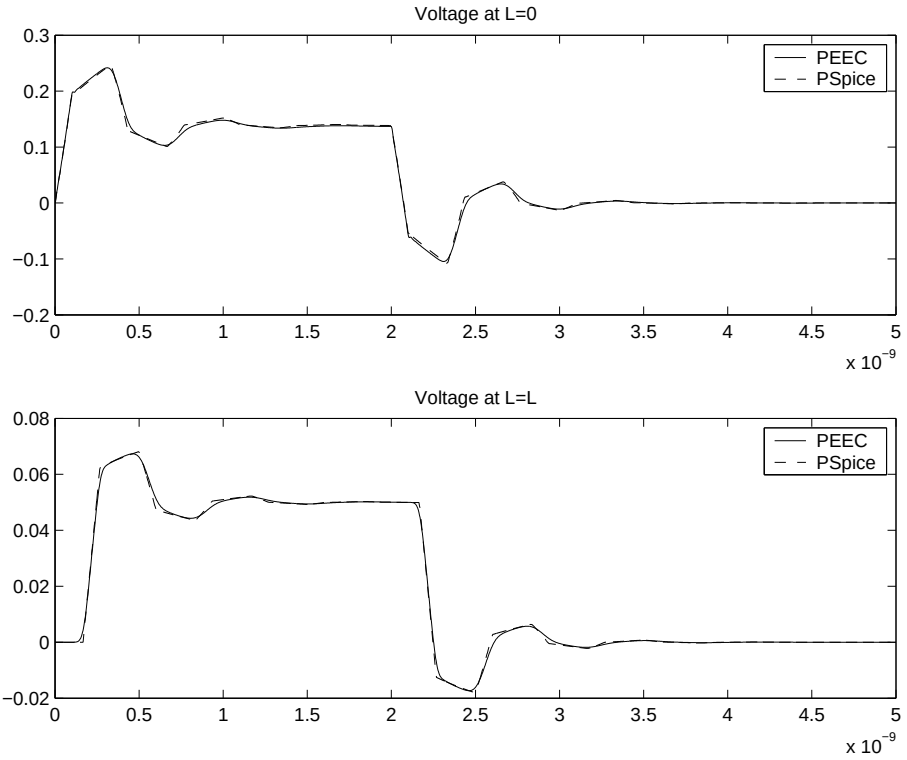

Figure 8: Near- and far-end response for TL. (L, P, R, τ, VFI)PEEC simulation.

The (VFI)PEEC simulation improved the results for the transmission line, as expected. However, the computational cost is high since the PEEC model consists of:

· 462 (82) capacitive nodes.

· 106491 (3321) part. mutual cop's.

· 860 (80) part. self inductances.

· 369370 (3160) part. mutual inductances.

With the previous PEEC model data, Fig. 7, within the parenthesis.

By reducing the time step to 1ps the results for the (VFI)PEEC simulation could be improved even more, Fig. 9. However, this simulation is unstable with a undamped oscillation starting at 3.5 ns.

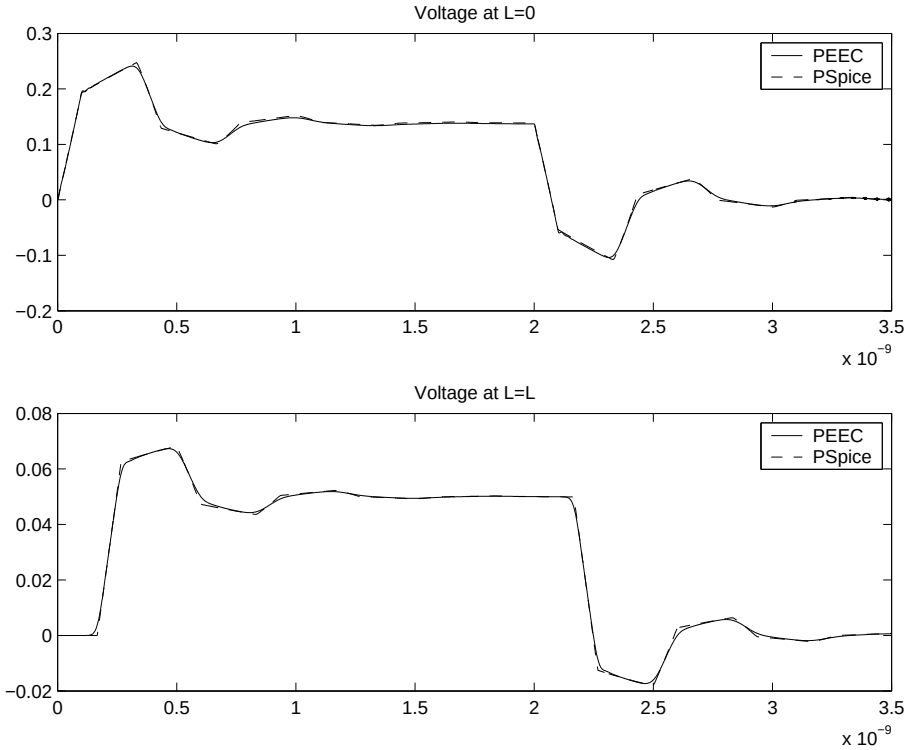

Figure 9: Near- and far-end response for TL. (L, P, R, τ, VFI)PEEC simulation. Time step = 1ps.

Bibliography

[1] H. Heeb and A. E. Ruehli. Approximate Time-Domain Models of Three-Dimensional Interconnects. In: *Proc. of the IEEE Int. Conference on Computer-Aided Design*, pages 201–205, Santa Clara, CA, USA, 1990.

[2] A. E. Ruehli. Inductance Calculations in a Complex Integrated Circuit Environment. *IBM Journal of Research and Development*, 16(5):470–481, September 1972.

[3] A. E. Ruehli and P. K. Wolff. Inductance Computations for Complex Three-Dimensional Geometries, In: *Proc. of the IEEE Int. Symposium on Circuits and Systems*, vol. 1, pages 16–19, New York, NY, 1981.

[4] C. Ho, A. Ruehli, and P. Brennan. The Modified Nodal Approach to Network Analysis. *IEEE Transactions on Circuits and Systems*, pages 504–509, June 1975.

[5] T. A. Jerse. A hybrid technique for efficiently estimating common mode currents in transmission-line structures. Ph.D. Dissertation, The University of Kentucky, 1994.

[6] J. E. Garrett. *Advancements of the Partial Element Equivalent Circuit Formulation.* Ph.D. Dissertation, The University of Kentucky, 1997.

[7] L. M. Wedepohl and L. Jackson. Modified Nodal Analysis: an essential addition to electrical circuit theory and analysis. *Engineering Science and Eduction Journal*, pages 84–92, June 2002.

[8] A. E. Djordjevic *et al. LINPAR for Windows: Matrix Parameters for Multiconductor Transmission Lines, Software and User's Manual, Version 2.0.* Artech House, July 1999.